Author Manuscript

Author Manuscript

Author Manuscript

Author Manuscript

HHS Public Access

Author manuscript

Clin Cancer Res. Author manuscript; available in PMC 2020 August 01.

Published in final edited form as:

Clin Cancer Res. 2020 February 01; 26(3): 679–689. doi:10.1158/1078-0432.CCR-19-2209.

Neoadjuvant PD-1 immune checkpoint blockade reverses functional immunodominance among tumor-antigen specific T cells

Jay Friedman[1], **Ellen C. Moore**[1], **Paul Zolkind**[2], **Yvette Robbins**[1], **Paul E. Clavijo**[1], **Lilian Sun**[1], **Sarah Greene**[1], **Megan Morisada**[1], **Wojciech Mydlarz**[3], **Nicole Schmitt**[3], **James Hodge**[4], **Hans Schreiber**[5], **Carter Van Waes**[6], **Ravindra Uppaluri**[7], **Clint T. Allen**[1,3]

[1]Translational Tumor Immunology Program, National Institute on Deafness and Other Communication Disorders, National Institutes of Health, Bethesda, MD

[2]Department of Otolaryngology-Head and Neck Surgery, Washington University in St. Louis, St. Louis, MO

[3]Department of Otolaryngology-Head and Neck Surgery, Johns Hopkins School of Medicine, Baltimore, MD

[4]Laboratory of Tumor Immunology and Biology, National Cancer Institute, National Institutes of Health, Bethesda, MD

[5]Department of Pathology, University of Chicago, Chicago, IL

[6]Tumor Biology Section, Head and Neck Surgery Branch, National Institute on Deafness and Other Communication Disorders, National Institutes of Health, Bethesda, MD

[7]Department of Surgery/Otolaryngology, Brigham and Women's Hospital and Dana-Farber Cancer Institute, Boston, MA

Abstract

Purpose—Surgical resection of primary tumor with regional lymphadenectomy remains the treatment of choice for patients with advanced human papillomavirus-negative head and neck squamous cell carcinoma. However, even when pathologic disease-free margins can be achieved, locoregional and/or distant disease relapse remains high. Perioperative immunotherapy may improve outcomes, but mechanistic data supporting the use of neoadjuvant or adjuvant treatment clinically is sparse.

Experimental design—Two syngeneic models of oral cavity carcinoma with defined T cell antigens were treated with PD-1 mAb before or after surgical resection of primary tumors, and antigen-specific T cell responses were explored with functional and *in vivo* challenge assays.

Results—We demonstrated that functional immunodominance developed among T cells targeting multiple independent tumor antigens. T cells specific for subdominant antigens

Corresponding Author: Clint T. Allen, MD, National Institutes of Health, 10 Center Drive, Room 7N240C, Bethesda, MD, 20892, Phone: 301-827-5620, clint.allen@nih.gov.

Conflict of interest: The authors have declared that no conflict of interest exists

Author Manuscript Author Manuscript Author Manuscript Author Manuscript

expressed greater levels of PD-1. Neoadjuvant, but not adjuvant, PD-1 immune checkpoint blockade broke immunodominance and induced T cell responses to dominant and subdominant antigens. Using tumors lacking the immunodominant antigen as a model of antigen escape, neoadjuvant PD-1 immune checkpoint blockade induced effector T cell immunity against tumor cells lacking immunodominant but retaining subdominant antigen. When combined with complete surgical excision, neoadjuvant PD-1 immune checkpoint blockade led to formation of immunologic memory capable of preventing engraftment of tumors lacking the immunodominant but retaining subdominant antigen.

Conclusions—Together, these results implicate PD-1 expression by T cells in the mechanism of functional immunodominance among independent T cell clones within a progressing tumor, and support the use of neoadjuvant PD-1 immune checkpoint blockade in patients with surgically resectable carcinomas.

Introduction

Surgical resection is a highly effective means of treating both early and advanced stage cancers, but half of all patients with advanced, human papillomavirus-negative head and neck squamous cell carcinoma will develop locoregional and/or distant relapse of disease following margin-negative resection(1). Once recurrence or distant metastasis occurs, prognosis is poor, even with the use of systemic immunotherapy such as programmed death receptor 1 (PD-1) immune checkpoint blockade(2,3). The rational use of neoadjuvant or adjuvant treatments to increase cure rates may carry the greatest chance of preventing disease relapse and improving survival.

Surgical resection of malignant disease removes a significant source of host immunosuppression and may reinvigorate dysfunctional tumor antigen-specific T cell responses that developed during carcinogenesis and cancer progression(4–6). However, the development of a polyclonal T cell response against multiple independent tumor antigens within a progressing tumor may nevertheless fail for multiple reasons. One such reason is suppression of T cell immunity targeting subdominant antigens by the presence of an immunodominant antigen(7–10). This has significant ramifications since immunoediting may lead to the loss of strong T cell antigens and the outgrowth of tumor cells expressing only subdominant antigens(11–13). Inducing polyclonal T cell responses against multiple antigens prior to surgical resection may enhance post-operative anti-tumor immunity and protect against recurrence of disease that has been immunoedited and lacks immunodominant antigens.

Exhausted CD8+ tumor infiltrating lymphocytes (TIL) that harbor T cell receptors (TCRs) specific for human leukocyte antigen (HLA)-restricted tumor antigens express PD-1(14,15). PD-1 immune checkpoint blockade rescues the function of tumor antigen-specific T cells that are suppressed by PD-1 expression(16). Recent data has demonstrated greater PD-1 expression on peripheral T cells specific for subdominant antigens in a model of polyclonal responses to multiple defined epitopes within a single model antigen(17). In this model system, PD-1 immune checkpoint blockade favored activation of PD-1+ T cells specific for subdominant epitopes. Whether the same findings would be true within the

Author Manuscript Author Manuscript Author Manuscript Author Manuscript

microenvironment of progressing cancers harboring multiple independent tumor antigens was unclear.

We sought to understand the role of PD-1 immune checkpoint blockade in the setting of progressing tumors harboring multiple independent T cell antigens. Using two syngeneic models of carcinogen-induced, human papillomavirus-negative oral cavity carcinomas, we established functional immunodominance patterns among independent T cell clones using tetramer staining and functional assays. Variable expression of PD-1 on different T cell clones appeared to contribute to functional immunodominance as PD-1 immune checkpoint blockade resulted in the activation of subdominant T cells and restored their ability to exert effector function against tumor cells lacking immunodominant antigen. We further demonstrated that neoadjuvant PD-1 immune checkpoint blockade combined with complete surgical excision induced effector immunity and durable immunologic memory. Mice were subsequently protected from engraftment of antigen loss variant tumors lacking immunodominant antigen. These results were not observed when PD-1 immune checkpoint blockade was administered in the adjuvant setting. Taken together, these results provide mechanistic insights into the development of functional immunodominance among T cell clones targeting independent antigens and support the use of neoadjuvant PD-1 immune checkpoint blockade in patients with surgically resectable malignancy.

Methods

Cells Culture

Original stocks of genomically characterized(18) parental mouse oral cancer 1 (pMOC1), MOC2, and MOC22 cells were maintained in culture as described(19). $MOC1_{ova}$ cells were generated by stable transduction of a pBABE backbone expression construct encoding for full-length ovalbumin via puromycin selection into pMOC1 as described(20). All cell lines were serially verified to be free of mycoplasma and other murine associated pathogens on a monthly basis and used at low (<30) passage number.

In Vivo Experiments

All *in vivo* experiments were performed in wild-type (WT) C57BL/6 (B6) mice under an Animal Care and Use Committee approved protocol. Tumors were stablished by subcutaneous injection of tumor cells (5×10^6) in Matrigel (30% by volume). All surgical resections were performed by the senior author (CTA) on anesthetized mice under sterile conditions. Primary tumors but not tumor draining lymph nodes were surgically excised at the time of tumor resection. Surgical wounds were closed with standard techniques using absorbable suture. Mice were administered meloxicam for analgesia after surgery for three days and monitored closely for changes in health in the post-operative setting. For all tumor cell challenge experiments, tumor cells (5×10^6) in Matrigel were injected subcutaneously in the contralateral flank. Mice were assessed for tumor growth three times weekly and tumor volume was calculated as: ($length^2$ x width)/2. PD-1 mAb (RMP1–14, *InVivo*Plus) or isotype control (2A3) were purchased from BioXCell and administered via intraperitoneal (IP) injection at 200 μg/injection in a total volume of 200 μL. Tumor-bearing mice were treated with neoadjuvant (days 7 and 10), adjuvant (days 17 and 20) or combination PD-1

Author Manuscript Author Manuscript Author Manuscript Author Manuscript

mAb. In some experiments, mice were euthanized and tumor draining lymph nodes and spleens were harvested for analysis 40 days after the initial primary tumor resection.

qRT-PCR

RNA was purified using the RNEasy Mini Kit (Qiagen). cDNA was synthesized utilizing a high capacity cDNA reverse transcription kit (Applied Biosystems). Relative expression of target genes compared to GAPDH was assessed on a Viia7 qPCR analyzer (Applied Biosystems). Custom primers to quantify p15E expression were synthesized by Integrated DNA Technologies: 5'-ATG GAA CCC GTC TCA CTA ACT CTG G and 3'-TCA CAG GGC CTG CAC TAC CGA AAT C.

Tumor infiltrating lymphocyte (TIL) culture

Tumors were harvested 14 days after implantation (tumor volume ~100 mm^3), divided into 1 mm fragments, and cultured in RPMI 1640-based media supplemented with recombinant murine IL-2 (100 units/mL). After 7 days of culture, TIL were harvested and enriched for CD3+ lymphocytes via negative magnetic selection (Mouse Pan T-cell Isolation Kit II, Miltenyi) on an AutoMACS Pro Separator (Miltenyi).

Flow cytometry

TIL were suspended in a 1% BSA solution and F_c receptor blockade was performed with CD16 mAb (Biolegend). Cells were first stained with tetramer for 20 min at 37°C, then stained with CD8 (clone KT15, MBL), CD44 (IM7), PD-1 (RPM1–14), Tim-3 (B8.2C12), CTLA-4 (UC10–4B9) and VISTA (MH5A) mAbs from Biolegend and LAG-3 (C9B7W) from eBioscience on ice for 45 min. $OVA_{257–264}$:H-$2K^b$ and $p15E_{604–611}$:H-$2K^b$ tetramers were purchased from MBL. The $mICAM_{308–315}$:H-$2K^b$ tetramer reagents were produced in the IML of CHIIPS at Washington University in St. Louis. Briefly, recombinant H-$2K^b$ and β2-microglobulin were produced in BL21-CodonPlus (DE3)-RIPL *Escherichia coli* (Agilent) and purified from inclusion bodies by size-exclusion FPLC as previously described(21). A UV-mediated exchange technique was used to generate peptide-specific monomers which were multimerized by streptavidin-conjugated PE as previously described(22). In other experiments, splenocytes were processed into single cell suspensions and subjected to RBC lysis. Whole splenocyte populations were exposed to peptides (1 μg/mL) corresponding to MHC class I restricted epitopes from p15E ($p15E_{604–611}$, KSPWFTTL, MBL), ovalbumin ($OVA_{257–264}$, SIINFEKL, InVivoGen) and mutant ICAM-1 ($mICAM_{308–315}$, TVYNFSAL, synthesized by Peptide 2.0) and rmIL-2 (100 U/mL) for 24 hours. Tetramer staining was performed with the addition of CD62L mAb (clone MEL-14, Biolegend). Antibodies for myeloid cell staining included CD45.2 (clone 104), CD11b (M1/70), F4/80 (BM8), Ly6C (HK1.4), Ly6G (1A8) and PD-L1 (MIH3) from Biolegend. FoxP3+ regulatory T cell staining was performed using the Mouse Regulatory T Cell Staining Kit #3 from eBioscience per manufacturer protocol. Non-viable cells were excluded with sytox blue (viable cells, Thermos) or zombie NIR (fixed cells, Biolegend) staining. Isotype control antibodies and fluorescence-minus-one approaches were used to ensure staining specificity. All analyses were performed on a BD Fortessa analyzer running FACSDiva software and interpreted using FlowJo (vX10.0.7r2).

Author Manuscript Author Manuscript Author Manuscript Author Manuscript

IFNγ production assays

Irradiated (20 Gy) WT B6 mouse splenocytes were pulsed with peptides (1 μg/mL) corresponding to MHC class I restricted epitopes for p15E, ovalbumin and mICAM and used as antigen presenting cells (APC). VSV-$N_{52–59}$ (RGYVYQGL) peptide was used as a control peptide. TIL and APC were co-cultured at a 1:2 effector:APC ratio for 24 hours. The number of IFNγ-producing TIL was determined by ELISpot (R&D Systems) or the magnitude of IFNγ production was determined by ELISA (R&D Systems) using manufacturer protocols. Spot counts for ELISpot assays were measured on an Immunospot ELISpot plate reader (Cellular Technology). In some experiments, T cells were isolated from tumor draining lymph nodes (TDLNs) via negative magnetic selection, and T cell antigen-specific responses were measured by IFNγ ELISA of 24-hour co-culture supernatants.

Impedance analysis

Real-time assessment of alteration in cell viability upon exposure to cultured TIL or cultured cytotoxic T-lymphocytes (CTL) was measured via impedance analysis as described(23). Briefly, tumor cells (1×10^4/well) were plated and allowed to adhere and gain impedance overnight. Following the addition of cultured TIL, a murine CTL line specific for $p15E_{604–611}$ (KSPWFTTL) presented on H-$2K^b$ (kind gift from Duane Hamilton, NCI, NIH) or OT-I CTL generated as described(23), alterations in impedance were assessed using the xCELLigence Real-Time Cell Analysis (RTCA) platform per manufacturer recommendations. Triton X-100 (0.2%) was used as a positive control for complete cell lysis. Percent loss of cell index was calculated as: 1 - (experimental cell index/control cell index) for a given timepoint. Mean values without standard deviation from at least two independent experiments are shown on impedance plots for clarity, with an adjacent box and whisker plot demonstrating mean +/− standard deviation at the 12 hour time point.

Statistics

Tests of significance between pairs of data are reported as p-values, derived using a student's t-test with a two-tailed distribution and calculated at 95% confidence. Comparison of multiple sets of data was achieved with analysis of variance (ANOVA) with Tukey's multiple comparisons. Differences in rates of tumor engraftment or survival between groups was determined by Log-Rank (Mantel-Cox) analysis. All error bars indicate standard deviation. Statistical significance was set to $p<0.05$. All analysis was performed using GraphPad Prism v7.

Results

pMOC1 oral carcinoma cells harbor an H-$2K^b$-restricted T cell antigen from the env protein of the endogenous retrovirus MuLV ($p15E_{604–611}$)(24,25). To establish a second known T cell antigen, pMOC1 cells were stably transfected with full length ovalbumin (OVA) to generate $MOC1_{ova}$. Expression of *p15E* in pMOC1 and $MOC1_{ova}$ cells was similar (Figure 1A). To verify that epitopes derived from p15E and OVA function as T cell antigens, pMOC1 and $MOC1_{ova}$ cells were co-cultured with CTL specific for $p15E_{604–611}$:H-$2K^b$ or $OVA_{257–264}$:H-$2K^b$. p15E-specific CTL killed pMOC1 and $MOC1_{ova}$ cells to a similar degree, and OVA-specific CTL killed $MOC1_{ova}$ cells but not pMOC1 cells (Supplementary

Author Manuscript Author Manuscript Author Manuscript Author Manuscript

Figure S1). To quantify the number of antigen-specific TIL within $MOC1_{ova}$ and pMOC1 tumors, tetramer staining of cultured TIL was performed (Figure 1B, validation of p15E tetramer specificity in Supplementary Figure S2). $MOC1_{ova}$ tumors harbored similar numbers of TIL specific for OVA and p15E. pMOC1 tumors harbored TIL specific for p15E only. TIL functional status was examined by antigen-specific IFNγ production with ELISpot. Although similar numbers of OVA- and p15E-specific TIL were present within $MOC1_{ova}$ tumors, a greater number of OVA-specific TIL produced higher levels of IFNγ compared to p15E-specific TIL (Figure 1C). Further, despite similar numbers of p15E-specific TIL present within $MOC1_{ova}$ and pMOC1 tumors, a greater number of p15E-specific TIL ($p<0.01$) within pMOC1 tumors produced IFNγ to a greater degree ($p<0.01$) compared to p15E-specific TIL within $MOC1_{ova}$ tumors (Figure 1D). These data suggested that p15E-specific TIL present within $MOC1_{ova}$ tumors are dysfunctional compared to p15E-specific TIL within pMOC1 tumors. Thus, the presence of OVA within MOC1 tumors appeared to suppress the function of p15E-specific TIL.

To test the functional consequences of dysfunctional p15E-specific TIL in $MOC1_{ova}$ tumors, co-culture experiments were performed to determine the cytolytic activity of $MOC1_{ova}$ TIL against pMOC1 tumor cells given similar levels of p15E expression and presentation. Although $MOC1_{ova}$ TIL effectively killed $MOC1_{ova}$ cells, they were less effective in killing pMOC1 cells (Figure 1E) demonstrating suppressed effector function. pMOC1 TIL controlled the growth of $MOC1_{ova}$ and pMOC1 cells to a similar degree. To determine if the presence of dysfunctional p15E-specific effector TIL within $MOC1_{ova}$ tumors affected immunologic memory after complete tumor resection, *in vivo* resection-rechallenge experiments were performed. Forty days after resection of $MOC1_{ova}$ tumors, mice were rechallenged with either $MOC1_{ova}$ or pMOC1 cells. Mice developed protective memory that prevented engraftment of new $MOC1_{ova}$ tumors upon challenge, but readily engrafted pMOC1 tumors despite p15E expression (Figure 1F). Mice challenged with pMOC1 cells after excision of day 14 pMOC1 tumors failed to engraft tumors (Figure 1G), suggesting that pMOC1 cells (lacking OVA) harbored one or more antigens capable of inducing immunologic memory. Thus, mice bearing $MOC1_{ova}$ tumors developed TIL with defective p15E-specific effector function failed to develop immunologic memory sufficient to reject challenge with pMOC1 tumor cells expressing p15E to a similar degree.

To explore possible mechanisms of reduced p15E-specific TIL function, cultured TIL cultured from $MOC1_{ova}$ tumors were phenotypically characterized by flow cytometry. At baseline, a greater percentage of p15E-specific TIL expressed greater levels (median fluorescent intensity) of PD-1 and Tim-3 than OVA-specific TIL but did not differ in the expression of CTLA-4, LAG-3 or VISTA (Figure 2A and Supplemental Figure 3A). Tetramer staining of TIL was performed after treatment *in vivo* with PD-1 mAb or isotype control. PD-1 mAb treatment of mice bearing $MOC1_{ova}$ tumors significantly expanded the number of TIL specific for both OVA and p15E (Figure 2B). By ELISpot assay, PD-1 mAb treatment enhanced the IFNγ production capacity of both OVA- and p15E-specific TIL (Figure 2C), suggesting that expanded, tetramer-positive, antigen-specific TIL were more functional. Co-culture of $MOC1_{ova}$ TIL with pMOC1 tumor cells revealed that TIL cultured from PD-1 mAb treated mice demonstrated greater ability to kill pMOC1 tumor cells compared to TIL cultured from mice treated with isotype control (Figure 2D). When

Author Manuscript Author Manuscript Author Manuscript Author Manuscript

analyzed by flow cytometry of fresh tumor digests, PD-1 mAb treatment of mice bearing $MOC1_{ova}$ tumors did not alter the infiltration of neutrophilic myeloid cells or FoxP3+ regulatory CD4+ T cells (Tregs) within the tumor microenvironment (Supplementary Figure S4A). These data suggested that *in vivo* PD-1 mAb treatment of mice bearing $MOC1_{ova}$ tumors enhanced the effector function of TIL targeting both OVA and p15E. PD-1 mAb treatment additionally rendered p15E-specific TIL, previously dysfunctional within tumors co-expressing OVA, functional and capable of exerting effector functions against p15E-expressing pMOC1 cells.

To determine the effects of *in vivo* PD-1 mAb treatment on the development of immunologic memory after complete tumor resection, further resection-rechallenge experiments were performed. Mice bearing $MOC1_{ova}$ tumors received two doses of neoadjuvant and adjuvant PD-1 mAb, alone or in combination, and were assessed for the ability to engraft pMOC1 tumors 40 days after tumor resection. Neoadjuvant PD-1 mAb administered before resection of tumor, alone or in combination with adjuvant PD-1 mAb, led to significantly reduced rates of pMOC1 tumor engraftment compared to control or adjuvant PD-1 mAb treatment alone (Figure 3A). These data suggested 1) that neoadjuvant PD-1 mAb before complete tumor resection is necessary and sufficient to induce immunologic memory capable of resisting tumor engraftment with tumor cells that lack OVA; and 2) that adjuvant PD-1 mAb given after complete tumor resection is incapable of producing the same results. To explore immune correlatives within secondary lymphoid organs after these treatments, T cells from tumor-draining lymph nodes (TDLNs) were assayed for antigen-specific IFNγ production 40 days after tumor resection. Upon exposure to antigenic peptides, IFNγ production was significantly greater in T cells sorted from TDLN of mice treated with neoadjuvant or combination PD-1 mAb compared to control or adjuvant treatment alone (Figure 3B). Peripheral antigen-specific T cells were assayed for quantity and memory phenotype. T cells in spleens of mice treated with neoadjuvant or combination PD-1 mAb harbored a significantly greater frequency of tetramer positive effector memory CD44+CD62L-CD8+ T cells compared to control or adjuvant treatment alone. Thus, neoadjuvant but not adjuvant PD-1 mAb treatment of mice bearing $MOC1_{ova}$ tumors resulted in the formation of immunologic memory that prevented engraftment of pMOC1 tumors lacking the OVA antigen.

The presence of OVA-specific CD8+ T cells in the naturally induced T cell repertoire of $MOC1_{ova}$ tumors appeared to inhibit the function of p15E-specific TIL. This was reversed with neoadjuvant but not adjuvant PD-1 mAb treatment. To ensure that these findings were not an artifact of an engineered OVA-expressing cancer model, we asked whether neoadjuvant PD-1 immune checkpoint blockade resulted in the same outcomes in a model with multiple naturally occurring antigens.

MOC22 oral carcinoma cells express an H-$2K^b$-restricted neoantigen derived from a mutated ICAM1 allele ($mICAM_{308–315}$)(26). PCR analysis revealed that MOC22 cells expressed p15E to a greater degree than pMOC1 cells (Figure 4A) and that p15E-secific CTL killed MOC22 cells to a greater degree than pMOC1 cells (Supplementary Figure S5). MOC22 tumors harbored TIL specific for both the mICAM neoantigen and p15E, whereas pMOC1 tumors lacked TIL specific for mICAM (Figure 4B). Assessing IFNγ production of MOC22

Author Manuscript Author Manuscript Author Manuscript Author Manuscript

TIL upon exposure to antigenic peptides revealed that a greater number of mICAM-specific TIL produced IFNγ compared to p15E-specific TIL despite there being a greater quantity of p15E-specific TIL present. Further, although MOC22 tumors have a significantly greater number of p15E-specific TIL by tetramer staining, these MOC22 TIL are less functional in both number ($p<0.01$) of IFNγ producing cells and degree ($p<0.01$) of IFNγ produced compared to p15E-specific TIL within pMOC1 tumors (Figures 4C and 4D). These data suggested that p15E-specific TIL present within MOC22 tumors are present but dysfunctional.

Co-culture experiments were performed to determine if MOC22 TIL could kill pMOC1 tumor cells. Although MOC22 TIL effectively killed MOC22 cells, they were less effective in killing pMOC1 cells (Figure 4E). pMOC1 TIL controlled the growth of MOC22 cells to a greater degree than pMOC1 cells. *In vivo* resection-challenge experiments revealed that after complete resection of MOC22 tumors, mice developed protective immunologic memory that prevented engraftment of new MOC22 tumors but readily engrafted pMOC1 tumors (Figure 4F).

At baseline, a greater percentage of p15E-specific TIL expressed PD-1 and Tim-3 to a greater degree (median fluorescent intensity) than mICAM-specific TIL but demonstrated similar or decreased expression of CTLA-4, LAG-3 or VISTA (Figure 5A and Supplemental Figure 3B). Tetramer staining of TIL revealed that PD-1 mAb treatment of mice bearing MOC22 tumors significantly expanded the number of TIL specific for both mICAM and p15E (Figure 5B). The number of functional mICAM- and p15E-specific TIL as determined by ELISpot increased as well (Fig. 5C). By ELISpot assay, PD-1 mAb treatment enhanced the function of both mICAM- and p15E-specific TIL (Figure 5C). PD-1 mAb treatment of mice bearing MOC22 tumors did not alter the infiltration of neutrophilic myeloid cells or Tregs within the tumor microenvironment (Supplementary Figure S3B). These data suggested that *in vivo* PD-1 mAb treatment of mice bearing MOC22 tumors enhanced both mICAM and p15E TIL effector function and rendered suppressed p15E-specific TIL to ones capable of killing pMOC1 cells.

Additional resection-rechallenge experiments were performed to explore how PD-1 mAb treatment altered the formation of immunologic memory in the MOC22-pMOC1 model system. Neoadjuvant PD-1 mAb administered before resection of MOC22 tumors, alone or in combination with adjuvant PD-1 mAb, led to significantly reduced rates of pMOC1 tumor engraftment upon challenge compared to control or adjuvant PD-1 mAb treatment alone (Figure 6A). Upon exposure to antigenic peptides, TDLN T cell IFNγ production was significantly greater in T cells sorted from TDLN of mice treated with neoadjuvant or combination PD-1 mAb compared to control or adjuvant treatment alone (Figure 6B). T cells in spleens of mice treated with neoadjuvant or combination PD-1 mAb harbored a significantly greater frequency of tetramer positive CD44+CD62L- CD8+ T cells, indicative of an effector memory phenotype, compared to control or adjuvant treatment alone. Thus, neoadjuvant but not adjuvant PD-1 mAb treatment of mice bearing MOC22 tumors resulted in the formation of immunologic memory that prevented engraftment of pMOC1 tumors lacking the mICAM neoantigen but expressing the shared p15E antigen.

Author Manuscript Author Manuscript Author Manuscript Author Manuscript

Discussion

The adaptive immune system faces multiple challenges within a progressing tumor. The presence of multiple independent T cell antigens leads to a hierarchy of responses where the presence of a dominant antigen or T cell clone often suppresses the function of other T cell clones specific for subdominant antigens(8,10,11). Here we established two model systems with multiple independent T cell antigens and established antigen dominance by exploring clonal expansion and antigen-specific function of TIL. In these specific models, the presence of T cell clones targeting either OVA or mICAM functionally suppressed T cells targeting p15E, establishing p15E as the subdominant antigen. This suppression of p15E-specific T cells appeared to be mediated at least in part by increased PD-1 expression. Therapeutic blockade of PD-1 enhanced the effector function of both dominant and subdominant T cell clones, rendering cultured TIL capable of killing antigen-loss variant tumor cells lacking the dominant antigen. This suggests that neoadjuvant PD-1 immune checkpoint blockade prior to removal of tumor relieves suppression of a polyclonal T cell response, reverses immunodominance, and allows immune activation within immunoedited tumors that no longer harbor cells expressing dominant antigens. Although most mice bearing progressing MOC22 tumors are cured with PD-1 mAb monotherapy(26), only 20–30% of mice bearing progressing $MOC1_{ova}$ tumors display significant tumor growth inhibition or tumor rejection(23). This is similar to the 15–20% of patients with recurrent/metastatic head and neck cancer that respond to PD-1 immune checkpoint blockade (2,3). The ability of PD-1 mAb treatment to reverse functional T cell immunodominance in $MOC1_{ova}$ tumors and for immunologic memory against multiple antigens to develop after surgery suggests that moving PD-1 immune checkpoint blockade into the neoadjuvant setting has the potential to benefit many patients with head and neck cancer.

Here, we offer evidence that functional immunodominance may be established in part by differential PD-1 expression among T cell clones. Although T cell clones targeting subdominant antigens also expressed greater levels of the immune checkpoint Tim-3, PD-1 mAb treatment was sufficient to recover their function. The precise mechanism(s) that confer increased PD-1 expression on T cell clones targeting subdominant antigens remain unclear. The ‘priority of first response’ theory suggests that the first T cell clone to engage the antigen:MHC complex for which it’s TCR is specific will clonally expand more than other T cell clones(8). Rather than demonstrating differential clonal expansion of T cell clones, we demonstrated that functional suppression of T cell clones targeting subdominant antigen involves PD-1 expression, making the ‘priority of first response’ theory unlikely in these specific models. TCR ligation drives PD-1 expression on antigen-experienced T cells through NFAT signaling(27). In both models, T cell clones specific for the endogenous murine retroviral antigen p15E were functionally suppressed via increased PD-1 expression. An alternative explanation is that increased TCR avidity of p15E-specific T cells may be driving increased PD-1 expression(28,29). Some studies have demonstrated low avidity of TCRs targeting the p15E antigen, but used IFN production as a readout of T cell function and did not explore PD-1 expression as a possible mechanism of decreased IFN responsiveness(30,31). Of note, the presence of T cell clones targeting endogenous retroviral antigen predicts positive responses to PD-1 immune checkpoint blockade(32), suggesting

Author Manuscript Author Manuscript Author Manuscript Author Manuscript

that blocking PD-1 signaling in T cells targeting retroviral antigens may be of biologic significance. Whether differential TCR avidity between T cell clones drives PD-1 expression and contributes to functional T cell dominance requires further study.

Liu et al. demonstrated that neoadjuvant depletion of Tregs and CD137 ligation induced greater immunologic control of metastases and improved survival compared to adjuvant treatment in pre-clinical models of metastatic breast carcinoma(33). Similar results could not be achieved with neoadjuvant chemotherapy, consistent with data demonstrating no survival advantage with neoadjuvant chemotherapy before surgical resection of head and neck cancer (34). Unlike neoadjuvant chemotherapy, neoadjuvant immunotherapy uses the tumor itself as an in-situ vaccine(35), possibly with increased cross-presentation of antigen and priming of new T cell clones. Liu et al. have also demonstrated enhanced survival of mice bearing metastatic breast carcinoma with neoadjuvant PD-1 mAb plus CD137 mAb(36). Here, we demonstrated that neoadjuvant PD-1 blockade alone was able to enhance the effector function of antigen-specific T cells independent of alterations in Treg tumor infiltration. FDA-approved PD-1 immune checkpoint blockade is widely available and currently more clinically relevant that other neoadjuvant immunotherapy approaches such as Treg depletion. Mechanistically, PD-1 signaling on T cells leads to downregulation of cell surface TCR function and/or expression(37). PD-1 blockade may lead to restored cell surface TCR function and/or expression on TIL, necessitating the presence of antigen:MHC complexes for TCR ligation and T cell activation. This is supported by multiple lines of evidence including the requirement for CD28 co-stimulatory molecule expression on T cells for rescue of function following PD-1 blockade(38) and the failure to develop protective immunity when other forms of immunotherapy are applied after complete tumor resection and removal of antigen(39). Thus, acute enhancement of effector T cell responses after PD-1 blockade may require the presence of tumor antigen for a period of time. This concept also requires further experimental study.

A separate line of investigation that impacts the timing of immune checkpoint blockade with extirpative surgery is the role of the tumor draining lymph nodes. Fransen et al. demonstrated that surgical removal of tumor draining but not contralateral lymph nodes abrogated T cell responses and tumor growth inhibition following PD-1 blockade(40). This suggests that PD-1 mAb treatment should be administered with tumor draining nodal basins intact. This has particular significance in the management of head and neck cancer where cervical nodal basins are often removed at the time of primary tumor resection due to regional metastasis of tumor(1), and further supports the use of PD-1 immune checkpoint blockade in the neoadjuvant setting.

In addition to enhancing polyclonal effector T cell responses against multiple antigens, neoadjuvant PD-1 blockade combined with complete surgical resection of tumor also resulted in the formation of effective immunologic memory to multiple antigens. This memory response did not form when adjuvant PD-1 mAb treatment was administered following complete resection of tumor despite the presence of antigen-specific T cell clones peripherally. This suggested that PD-1 blockade in the presence of tumor antigen (neoadjuvant) is required to enhance polyclonal effector function, and that removal of antigen (surgical excision) enables effective contraction of effector T cells into memory T

Author Manuscript Author Manuscript Author Manuscript Author Manuscript

cells. This precisely mirrors events that occur with an acute viral infection, where effector to memory T cell contraction occurs following immune-mediated clearance of viral antigen(41). Chronic persistence of antigen throughout different phases of T cell responses, as occurs in the presence of persistent tumor, is highly immunosuppressive(42). Additional sources of immunosuppression arise from the tumor microenvironment, and removal of large volume malignant disease may enhance effector responses enhance against smaller deposits of residual disease(43).

Formation of durable antigen-specific immunologic memory may protect against development of a new or recurrent malignancy with shared antigens(44–46). However, a limitation of the models used in this study is that complete surgical excision does not model the clinical dilemma of minimal residual disease after incomplete surgical excision or the presence of metastasis at the time of surgery. Given the very high recurrence rate of head and neck cancer, it is hypothesized that many patients harbor minimal residual disease or subclinical metastatic disease after a pathologically margin-negative resection(1,47). Whether enhancement of effector T cell responses sufficient to eliminate minimal residual or micro-metastatic disease occurs with neoadjuvant PD-1 blockade requires further study, and the development of head and neck cancer models that harbor T cell antigens but also spontaneously metastasize to allow study of this clinical scenario is ongoing. Another limitation of this work is our inability to conclude whether the same results of long-lasting protective anti-tumor immunity would occur in the setting of induction PD-1 immune checkpoint blockade followed by curative concurrent chemoradiation treatment. An additional limitation of our work is a lack of phenotypic characterization of TIL following 7 days of culture in these models. Emerging data demonstrates that the differentiation status of TIL may influence effector function(48). Assessment of day 7 TIL in these models with techniques such as single cell RNA sequencing could provide insight into how PD-1 mAb treatment influences T cell differentiation of cultured TIL.

Neoadjuvant or adjuvant treatments may enhance the curative potential of surgical resection of malignancy, especially in late-stage tumors where locoregional or distant failure rates are high. Indeed, early reports on the use of single agent neoadjuvant PD-1 immune checkpoint blockade in patients with melanoma and lung cancer have demonstrated promising results with high rates of clinical-to-pathologic downstaging and even complete regression of tumor in subsets of patients(49,50). Mechanistic pre-clinical data supporting the use of immunotherapy in combination with surgery is critical as any potential patient benefit needs to outweigh the risk of immune-related adverse events. This is especially true in the neoadjuvant setting where an adverse event could delay surgery. Here, we demonstrated that neoadjuvant PD-1 blockade monotherapy reversed functional immunodominance and induced polyclonal T cell responses to enhance effector immunity against tumor cells both harboring and lacking dominant antigens. Additionally, neoadjuvant, but not adjuvant, PD-1 blockade allowed for the formation of effective immunologic memory that protected mice from engraftment of tumors lacking dominant antigens. Given that progressing tumors are subject to immunoediting and that antigen loss variants represent a major obstacle to effective T cell-based immunotherapy, these results strongly support the use of PD-1 immune checkpoint blockade in the neoadjuvant setting.

Author Manuscript Author Manuscript Author Manuscript Author Manuscript

Supplementary Material

Refer to Web version on PubMed Central for supplementary material.

Acknowledgements

J. Friedman, E. Moore, Y. Robbins, P. Clavijo, L. Sun and C. Allen were supported by the Intramural Research Program of the NIH, NIDCD, project number ZIA-DC000087. S. Greene and M. Morisada were supported through the NIH Medical Research Scholars Program, a public-private partnership supported jointly by the NIH and contributions to the Foundation for the NIH from the Doris Duke Charitable Foundation (DDCF Grant #2014194), the American Association for Dental Research, the Colgate-Palmolive Company, Genentech, Elsevier, and other private donors. R. Uppaluri was supported by NIH/NIDCR DE027736.

References

1. Bernier J, Domenge C, Ozsahin M, Matuszewska K, Lefebvre JL, Greiner RH, et al. Postoperative irradiation with or without concomitant chemotherapy for locally advanced head and neck cancer. N Engl J Med 2004;350(19):1945–52. [PubMed: 15128894]
2. Ferris RL, Blumenschein G Jr., Fayette J, Guigay J, Colevas AD, Licitra L, et al. Nivolumab for Recurrent Squamous-Cell Carcinoma of the Head and Neck. The New England journal of medicine 2016;375(19):1856–67. [PubMed: 27718784]
3. Seiwert TY, Burtness B, Mehra R, Weiss J, Berger R, Eder JP, et al. Safety and clinical activity of pembrolizumab for treatment of recurrent or metastatic squamous cell carcinoma of the head and neck (KEYNOTE-012): an open-label, multicentre, phase 1b trial. The Lancet Oncology 2016;17(7):956–65. [PubMed: 27247226]
4. Bursuker I, North RJ. Immunological consequences of tumor excision: from active immunity to immunological memory. Int J Cancer 1986;37(2):275–81. [PubMed: 3943923]
5. Salvadori S, Martinelli G, Zier K. Resection of solid tumors reverses T cell defects and restores protective immunity. J Immunol 2000;164(4):2214–20. [PubMed: 10657677]
6. Danna EA, Sinha P, Gilbert M, Clements VK, Pulaski BA, Ostrand-Rosenberg S. Surgical removal of primary tumor reverses tumor-induced immunosuppression despite the presence of metastatic disease. Cancer Res 2004;64(6):2205–11. [PubMed: 15026364]
7. Van Waes C, Monach PA, Urban JL, Wortzel RD, Schreiber H. Immunodominance deters the response to other tumor antigens thereby favoring escape: prevention by vaccination with tumor variants selected with cloned cytolytic T cells in vitro. Tissue Antigens 1996;47(5):399–407. [PubMed: 8795140]
8. Rowley DA, Stach RM. A first or dominant immunization. I. Suppression of simultaneous cytolytic T cell responses to unrelated alloantigens. J Exp Med 1993;178(3):835–40. [PubMed: 8350057]
9. Seung S, Urban JL, Schreiber H. A tumor escape variant that has lost one major histocompatibility complex class I restriction element induces specific CD8+ T cells to an antigen that no longer serves as a target. J Exp Med 1993;178(3):933–40. [PubMed: 8394406]
10. Sandberg JK, Grufman P, Wolpert EZ, Franksson L, Chambers BJ, Karre K. Superdominance among immunodominant H-2Kb-restricted epitopes and reversal by dendritic cell-mediated antigen delivery. J Immunol 1998;160(7):3163–9. [PubMed: 9531271]
11. Wortzel RD, Urban JL, Philipps C, Fitch FW, Schreiber H. Independent immunodominant and immunorecessive tumor-specific antigens on a malignant tumor: antigenic dissection with cytolytic T cell clones. J Immunol 1983;130(5):2461–6. [PubMed: 6187859]
12. Urban JL, Kripke ML, Schreiber H. Stepwise immunologic selection of antigenic variants during tumor growth. J Immunol 1986;137(9):3036–41. [PubMed: 3489784]
13. Schreiber RD, Old LJ, Smyth MJ. Cancer immunoediting: integrating immunity's roles in cancer suppression and promotion. Science 2011;331(6024):1565–70. [PubMed: 21436444]
14. Gros A, Robbins PF, Yao X, Li YF, Turcotte S, Tran E, et al. PD-1 identifies the patient-specific CD8(+) tumor-reactive repertoire infiltrating human tumors. J Clin Invest 2014;124(5):2246–59. [PubMed: 24667641]

Author Manuscript Author Manuscript Author Manuscript Author Manuscript

15. Wei SC, Duffy CR, Allison JP. Fundamental Mechanisms of Immune Checkpoint Blockade Therapy. Cancer Discov 2018;8(9):1069–86. [PubMed: 30115704]
16. Tumeh PC, Harview CL, Yearley JH, Shintaku IP, Taylor EJ, Robert L, et al. PD-1 blockade induces responses by inhibiting adaptive immune resistance. Nature 2014;515(7528):568–71. [PubMed: 25428505]
17. Memarnejadian A, Meilleur CE, Shaler CR, Khazaie K, Bennink JR, Schell TD, et al. PD-1 Blockade Promotes Epitope Spreading in Anticancer CD8(+) T Cell Responses by Preventing Fratricidal Death of Subdominant Clones To Relieve Immunodomination. J Immunol 2017;199(9): 3348–59. [PubMed: 28939757]
18. Onken MD, Winkler AE, Kanchi KL, Chalivendra V, Law JH, Rickert CG, et al. A surprising cross-species conservation in the genomic landscape of mouse and human oral cancer identifies a transcriptional signature predicting metastatic disease. Clin Cancer Res 2014;20(11):2873–84. [PubMed: 24668645]
19. Judd NP, Winkler AE, Murillo-Sauca O, Brotman JJ, Law JH, Lewis JS Jr., et al. ERK1/2 regulation of CD44 modulates oral cancer aggressiveness. Cancer Res 2012;72(1):365–74. [PubMed: 22086849]
20. Morisada M, Moore EC, Hodge R, Friedman J, Cash HA, Hodge JW, et al. Dose-dependent enhancement of T-lymphocyte priming and CTL lysis following ionizing radiation in an engineered model of oral cancer. Oral Oncol 2017;71:87–94. [PubMed: 28688697]
21. Ribas A, Shin DS, Zaretsky J, Frederiksen J, Cornish A, Avramis E, et al. PD-1 Blockade Expands Intratumoral Memory T Cells. Cancer Immunol Res 2016;4(3):194–203. [PubMed: 26787823]
22. Ott PA, Hu Z, Keskin DB, Shukla SA, Sun J, Bozym DJ, et al. An immunogenic personal neoantigen vaccine for patients with melanoma. Nature 2017;547(7662):217–21. [PubMed: 28678778]
23. Sun L, Moore E, Berman R, Clavijo PE, Saleh A, Chen Z, et al. WEE1 kinase inhibition reverses G2/M cell cycle checkpoint activation to sensitize cancer cells to immunotherapy. Oncoimmunology 2018;7(10):e1488359. [PubMed: 30288354]
24. Huang AY, Gulden PH, Woods AS, Thomas MC, Tong CD, Wang W, et al. The immunodominant major histocompatibility complex class I-restricted antigen of a murine colon tumor derives from an endogenous retroviral gene product. Proc Natl Acad Sci U S A 1996;93(18):9730–5. [PubMed: 8790399]
25. Nagaya T, Friedman J, Maruoka Y, Ogata F, Okuyama S, Clavijo PE, et al. Host Immunity Following Near-Infrared Photoimmunotherapy Is Enhanced with PD-1 Checkpoint Blockade to Eradicate Established Antigenic Tumors. Cancer Immunol Res 2019;7(3):401–13. [PubMed: 30683733]
26. Zolkind P, Przybylski D, Marjanovic N, Nguyen L, Lin T, Johanns T, et al. Cancer immunogenomic approach to neoantigen discovery in a checkpoint blockade responsive murine model of oral cavity squamous cell carcinoma. Oncotarget 2018;9(3):4109–19. [PubMed: 29423108]
27. Martinez GJ, Pereira RM, Aijo T, Kim EY, Marangoni F, Pipkin ME, et al. The transcription factor NFAT promotes exhaustion of activated CD8(+) T cells. Immunity 2015;42(2):265–78. [PubMed: 25680272]
28. Simon S, Vignard V, Florenceau L, Dreno B, Khammari A, Lang F, et al. PD-1 expression conditions T cell avidity within an antigen-specific repertoire. Oncoimmunology 2016;5(1):e1104448. [PubMed: 26942093]
29. Wherry EJ, Ha SJ, Kaech SM, Haining WN, Sarkar S, Kalia V, et al. Molecular signature of CD8+ T cell exhaustion during chronic viral infection. Immunity 2007;27(4):670–84. [PubMed: 17950003]
30. Zeh HJ 3rd, Perry-Lalley D, Dudley ME, Rosenberg SA, Yang JC. High avidity CTLs for two self-antigens demonstrate superior in vitro and in vivo antitumor efficacy. J Immunol 1999;162(2):989–94. [PubMed: 9916724]
31. Shitaoka K, Hamana H, Kishi H, Hayakawa Y, Kobayashi E, Sukegawa K, et al. Identification of Tumoricidal TCRs from Tumor-Infiltrating Lymphocytes by Single-Cell Analysis. Cancer Immunol Res 2018;6(4):378–88. [PubMed: 29475880]

Author Manuscript Author Manuscript Author Manuscript Author Manuscript

32. Smith CC, Beckermann KE, Bortone DS, De Cubas AA, Bixby LM, Lee SJ, et al. Endogenous retroviral signatures predict immunotherapy response in clear cell renal cell carcinoma. J Clin Invest 2018;128(11):4804–20. [PubMed: 30137025]
33. Liu J, Blake SJ, Yong MC, Harjunpaa H, Ngiow SF, Takeda K, et al. Improved Efficacy of Neoadjuvant Compared to Adjuvant Immunotherapy to Eradicate Metastatic Disease. Cancer Discov 2016;6(12):1382–99. [PubMed: 27663893]
34. Licitra L, Grandi C, Guzzo M, Mariani L, Lo Vullo S, Valvo F, et al. Primary chemotherapy in resectable oral cavity squamous cell cancer: a randomized controlled trial. J Clin Oncol 2003;21(2):327–33. [PubMed: 12525526]
35. Melero I, Berraondo P, Rodriguez-Ruiz ME, Perez-Gracia JL. Making the Most of Cancer Surgery with Neoadjuvant Immunotherapy. Cancer Discov 2016;6(12):1312–4. [PubMed: 27920139]
36. Liu J, Rozeman EA, O'Donnell JS, Allen S, Fanchi L, Smyth MJ, et al. Batf3(+) DCs and type I IFN are critical for the efficacy of neoadjuvant cancer immunotherapy. Oncoimmunology 2019;8(2):e1546068. [PubMed: 30713806]
37. Karwacz K, Bricogne C, MacDonald D, Arce F, Bennett CL, Collins M, et al. PD-L1 co-stimulation contributes to ligand-induced T cell receptor down-modulation on CD8+ T cells. EMBO Mol Med 2011;3(10):581–92. [PubMed: 21739608]
38. Kamphorst AO, Wieland A, Nasti T, Yang S, Zhang R, Barber DL, et al. Rescue of exhausted CD8 T cells by PD-1-targeted therapies is CD28-dependent. Science 2017;355(6332):1423–7. [PubMed: 28280249]
39. Broomfield S, Currie A, van der Most RG, Brown M, van Bruggen I, Robinson BW, et al. Partial, but not complete, tumor-debulking surgery promotes protective antitumor memory when combined with chemotherapy and adjuvant immunotherapy. Cancer Res 2005;65(17):7580–4. [PubMed: 16140921]
40. Fransen MF, Schoonderwoerd M, Knopf P, Camps MG, Hawinkels LJ, Kneilling M, et al. Tumor-draining lymph nodes are pivotal in PD-1/PD-L1 checkpoint therapy. JCI Insight 2018;3(23) doi 10.1172.
41. Wherry EJ, Ahmed R. Memory CD8 T-cell differentiation during viral infection. J Virol 2004;78(11):5535–45. [PubMed: 15140950]
42. Shin H, Wherry EJ. CD8 T cell dysfunction during chronic viral infection. Curr Opin Immunol 2007;19(4):408–15. [PubMed: 17656078]
43. Judy BF, Singhal S. How can cytoreduction surgery improve the prospects for cancer patients receiving immunotherapy? Immunotherapy 2012;4(11):1077–80. [PubMed: 23194354]
44. Dhodapkar K, Dhodapkar M. Harnessing shared antigens and T-cell receptors in cancer: Opportunities and challenges. Proceedings of the National Academy of Sciences of the United States of America 2016;113(29):7944–5. [PubMed: 27410048]
45. Laban S, Giebel G, Klumper N, Schrock A, Doescher J, Spagnoli G, et al. MAGE expression in head and neck squamous cell carcinoma primary tumors, lymph node metastases and respective recurrences-implications for immunotherapy. Oncotarget 2017;8(9):14719–35. [PubMed: 28146422]
46. Van Waes C, Urban JL, Rothstein JL, Ward PL, Schreiber H. Highly malignant tumor variants retain tumor-specific antigens recognized by T helper cells. J Exp Med 1986;164(5):1547–65. [PubMed: 2945891]
47. Partridge M, Brakenhoff R, Phillips E, Ali K, Francis R, Hooper R, et al. Detection of rare disseminated tumor cells identifies head and neck cancer patients at risk of treatment failure. Clin Cancer Res 2003;9(14):5287–94. [PubMed: 14614011]
48. Hinrichs CS, Borman ZA, Cassard L, Gattinoni L, Spolski R, Yu Z, et al. Adoptively transferred effector cells derived from naive rather than central memory CD8+ T cells mediate superior antitumor immunity. Proc Natl Acad Sci U S A 2009;106(41):17469–74. [PubMed: 19805141]
49. Huang AC, Orlowski RJ, Xu X, Mick R, George SM, Yan PK, et al. A single dose of neoadjuvant PD-1 blockade predicts clinical outcomes in resectable melanoma. Nat Med 2019;25(3):454–61. [PubMed: 30804515]

Author Manuscript Author Manuscript Author Manuscript Author Manuscript

50. Forde PM, Chaft JE, Smith KN, Anagnostou V, Cottrell TR, Hellmann MD, et al. Neoadjuvant PD-1 Blockade in Resectable Lung Cancer. N Engl J Med 2018;378(21):1976–86. [PubMed: 29658848]

Author Manuscript Author Manuscript Author Manuscript Author Manuscript

Translational relevance

Preliminary results from perioperative immune checkpoint blockade are promising, but mechanistic data supporting neoadjuvant versus adjuvant treatment is needed. Using syngeneic models of carcinoma with defined antigenicity, we found that neoadjuvant programmed death receptor-1 (PD-1) immune checkpoint blockade led to reversal of functional immunodominance among T cell clones targeting independent antigens, and allowed the formation immunological memory capable of rejecting tumor cell challenge after surgical resection of tumors. These results were not observed with adjuvant immune checkpoint blockade. These results support the use of neoadjuvant immune checkpoint blockade administered before resection of malignancy, and will guide the development of clinical trials employing up front immunotherapy in combination with surgery in patients with resectable carcinomas.

Author Manuscript Author Manuscript Author Manuscript Author Manuscript

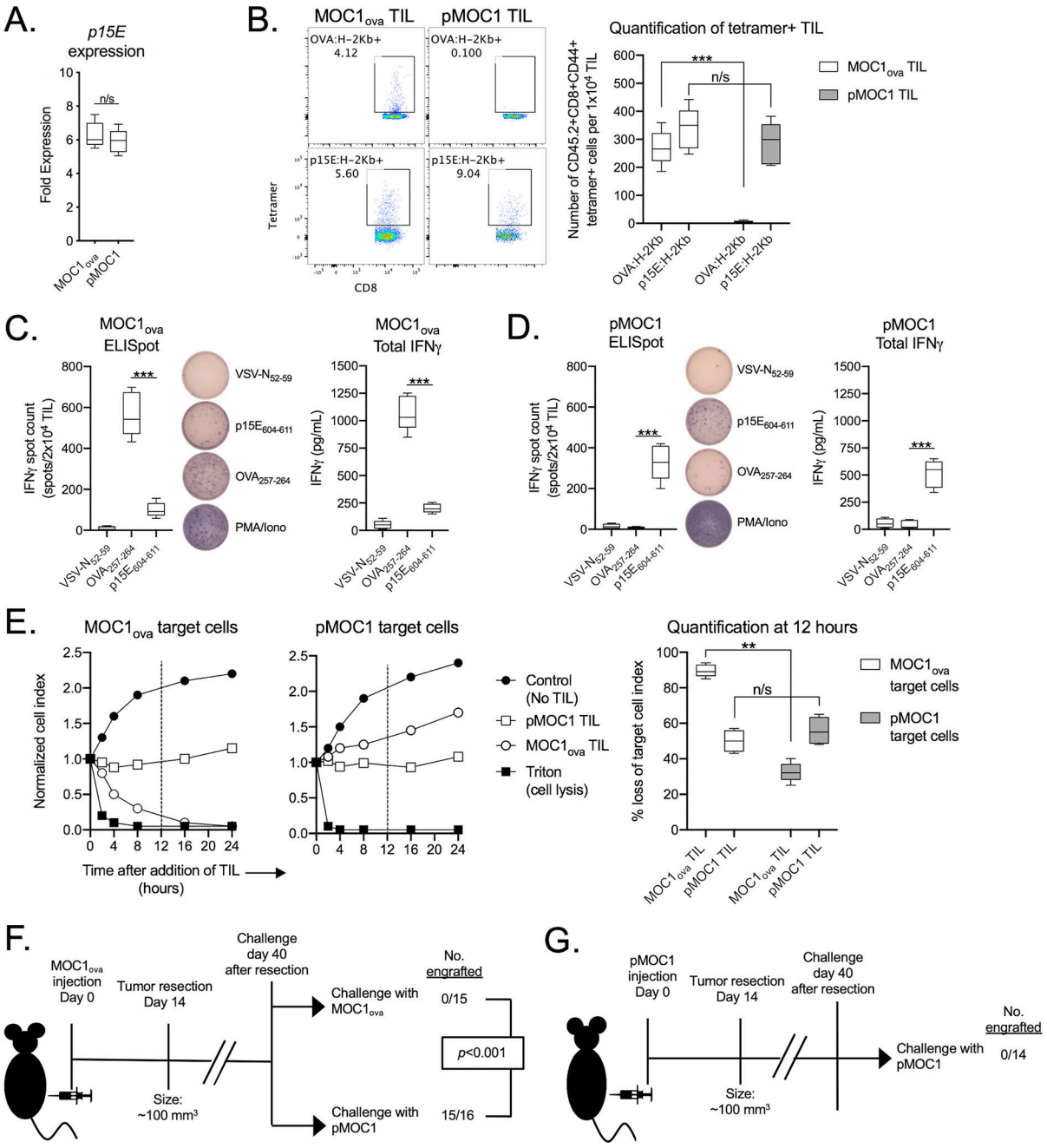

Figure 1 –. Functional TIL targeting p15E failed to develop in the presence of OVA

A, qPCR was used to measure *p15E* gene expression in $MOC1_{ova}$ and pMOC1 cells. *p15E* expression in MOC2 cells was used as a reference and set to 1.

B, TIL were cultured from day 14 $MOC1_{ova}$ or pMOC1 tumors. After 7 days in culture, TIL were assessed for tetramer positivity by flow cytometry. Representative dot plots are shown on the left. Quantity of tetramer positive TIL is shown on the right ($n = 5$ independent tumors each model).

C and **D**, TIL cultured from $MOC1_{ova}$ tumors (**C**) or pMOC1 tumors (**D**) were assessed for IFNγ production upon exposure to control ($VSV\text{-}N_{52–59}$) or antigenic peptides ($OVA_{257–264}$

Author Manuscript Author Manuscript Author Manuscript Author Manuscript

and $p15E_{604–611}$). Number of IFNγ producing cells was quantified by ELISpot (left, with representative photomicrographs of wells) and cumulative production of IFNγ was quantified by ELISA (right) ($n = 5$ independent tumors each model).

E, TIL cultured from day 14 $MOC1_{ova}$ or pMOC1 tumors were co-cultured with $MOC1_{ova}$ or pMOC1 target cells and loss of target cell viability was assessed in real-time by impedance analysis. Representative impedance plots are shown on the left. Quantification of loss of target cell index 12 hours after initiation of co-culture (vertical dashed line) is shown on the right (TIL pooled from 5 independent tumors each model).

F, $MOC1_{ova}$ tumors were established in WT B6 mice and completely resected at day 14. Forty days after resection, mice were challenged with either $MOC1_{ova}$ or pMOC1 cells and followed for tumor engraftment. Cumulative data from three independent experiments. Significance determined by Mantel-Cox analysis.

G, pMOC1 tumors were established in WT B6 mice and completely resected at day 14. Forty days after resection, mice were challenged with pMOC1 cells and followed for tumor engraftment. Cumulative data from two independent experiments.

Unless stated otherwise, all data shown is representative data from one of at least two independent experiments.

**, $p < 0.01$; ***, $p < 0.001$, student's t-test; n/s, non-significant.

Author Manuscript Author Manuscript Author Manuscript Author Manuscript

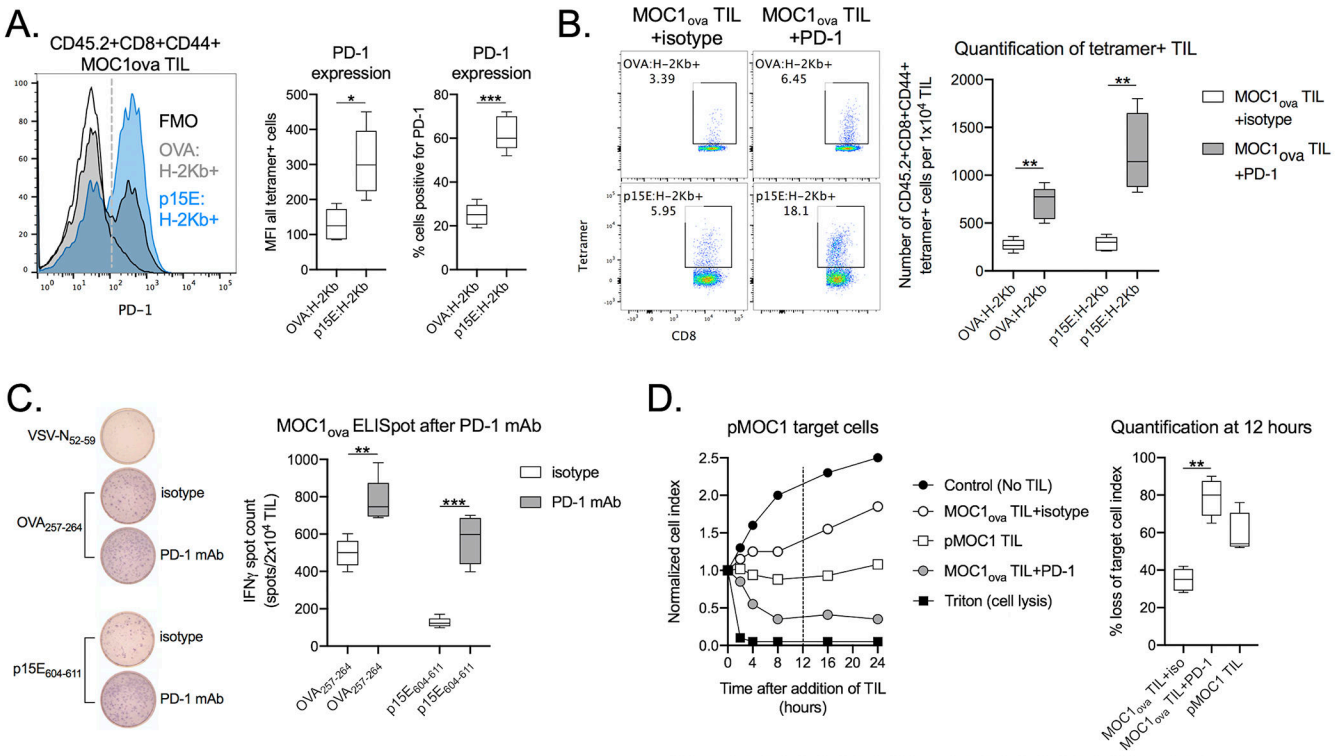

Figure 2 –. PD-1 mAb restored the function of TIL targeting p15E in MOC1$_{ova}$ tumors

A, MOC1$_{ova}$ TIL specific for OVA:H-2K^b or p15E:H-2K^b were assessed for PD-1 expression by flow cytometry. Representative histogram of PD-1 staining is shown on the left, with qualification of PD-1 expression on all tetramer positive cells (median fluorescent intensity) as well as the percentage of positive cells (dashed grey line) shown on the right (n = 5 independent tumors).

B, WT B6 mice bearing MOC1$_{ova}$ tumors were treated with PD-1 mAb or isotype control (days 7 and 10). TIL were cultured from day 14 tumors, and after 7 days of culture, TIL were assessed for tetramer positivity by flow cytometry. Representative dot plots are shown on the left. Quantity of tetramer positive TIL is shown on the right (n = 5 independent tumors each condition).

C, TIL cultured from day 14 MOC1$_{ova}$ tumors treated with PD-1 mAb or isotype control were assessed for IFNγ production upon exposure to antigenic peptides by ELISpot. Representative photomicrographs of ELISpot wells are shown on the left, with quantification of spot counts on the right (n = 5 independent tumors each condition).

D, TIL cultured from day 14 MOC1$_{ova}$ tumors treated with PD-1 mAb or isotype control were co-cultured with pMOC1 target cells and loss of target cell viability was assessed by impedance analysis. Representative impedance plot is shown on the left. Quantification of loss of target cell index 12 hours after initiation of co-culture (vertical dashed line) is shown on the right (TIL pooled from 5 independent tumors each condition).

All data shown is representative data from one of at least two independent experiments.

*, $p < 0.05$; **, $p < 0.01$; ***, $p < 0.001$, student's t-test

Author Manuscript Author Manuscript Author Manuscript Author Manuscript

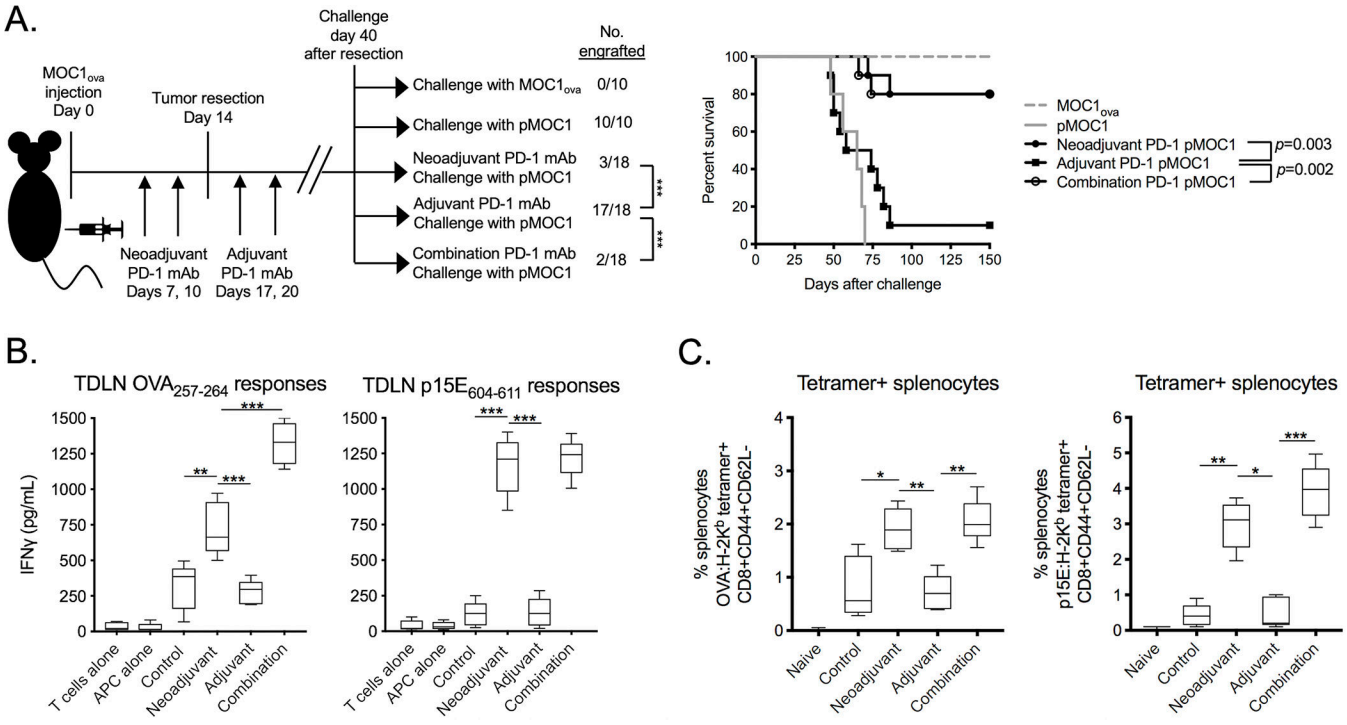

Figure 3 –. Mice rejected engraftment with tumor cells lacking OVA following neoadjuvant PD-1 mAb

A, $MOC1_{ova}$ tumors were established in WT B6 mice and completely resected at day 14. Tumor-bearing mice were given neoadjuvant (days 7 and 10), adjuvant (days 17 and 20) or combination PD-1 mAb. 40 days after resection, untreated mice were challenged with $MOC1_{ova}$ or pMOC1 cells as controls, and treated mice were challenged with pMOC1 cells and followed for engraftment. Tumor engraftment rates are shown on the left, and survival to 150 days after challenge is shown as a Kaplan-Meier curve on the right. Cumulative data from two independent experiments.

B and **C**, $MOC1_{ova}$ tumor-bearing mice were treated neoadjuvant, adjuvant or combination PD-1 mAb as in A. **B**, 40 days after resection, T cells were sorted form tumor draining lymph nodes (TDLN) and assessed for IFNγ production upon exposure to antigenic peptides by ELISA. **C**, 40 days after resection, splenic T cells were assessed for tetramer and memory marker positivity by flow cytometry ($n = 5$ independent tumors each condition). Unless stated otherwise, all data shown is representative data from one of at least two independent experiments.

*, $p < 0.05$; **, $p < 0.01$; ***, $p < 0.001$, student's t-test

Author Manuscript
Author Manuscript
Author Manuscript
Author Manuscript

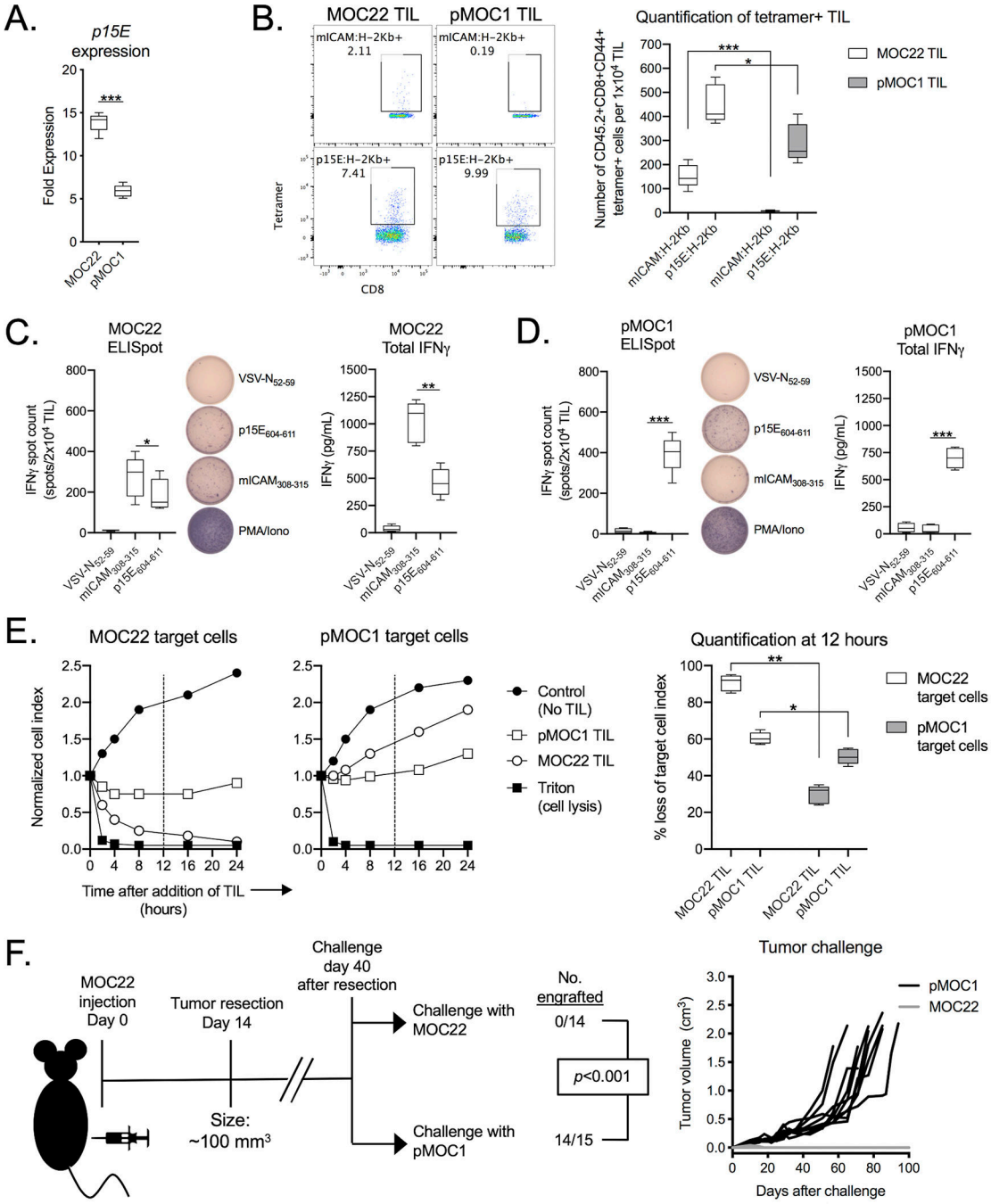

Figure 4 –. Functional TIL targeting p15E failed to develop in the presence of mICAM

A, qPCR was used to measure *p15E* gene expression in MOC22 and pMOC1 cells.

B, TIL were cultured from day 14 MOC22 or pMOC1 tumors. After 7 days in culture, TIL were assessed for tetramer positivity by flow cytometry. Representative dot plots are shown on the left. Quantity of tetramer positive TIL is shown on the right (n = 5 independent tumors each model).

C and **D**, TIL cultured from MOC22 tumors (**C**) or pMOC1 tumors (**D**) were assessed for IFNγ production upon exposure to control (VSV-$N_{52–59}$) or antigenic peptides

Author Manuscript Author Manuscript Author Manuscript Author Manuscript

($mICAM_{308-315}$ and $p15E_{604–611}$). Number of IFNγ producing cells was quantified by ELISpot (left, with representative photomicrographs of wells) and cumulative production of IFNγ was quantified by ELISA (right) ($n = 5$ independent tumors each model).

E, TIL cultured from day 14 MOC22 or pMOC1 tumors were co-cultured with MOC22 or pMOC1 target cells and loss of target cell viability was assessed in real-time by impedance analysis. Representative impedance plots are shown on the left. Quantification of loss of target cell index 12 hours after initiation of co-culture (vertical dashed line) is shown on the right (TIL pooled from 5 independent tumors each model).

F, MOC22 tumors were established in WT B6 mice and completely resected at day 14. 40 days after resection, mice were challenged with either MOC22 or pMOC1 cells and followed for tumor engraftment. Cumulative data from two independent experiments. Significance determined by Mantel-Cox analysis.

Unless stated otherwise, all data shown is representative data from one of at least two independent experiments.

*, $p < 0.05$; **, $p < 0.01$; ***, $p < 0.001$; student's t-test

Author Manuscript Author Manuscript Author Manuscript Author Manuscript

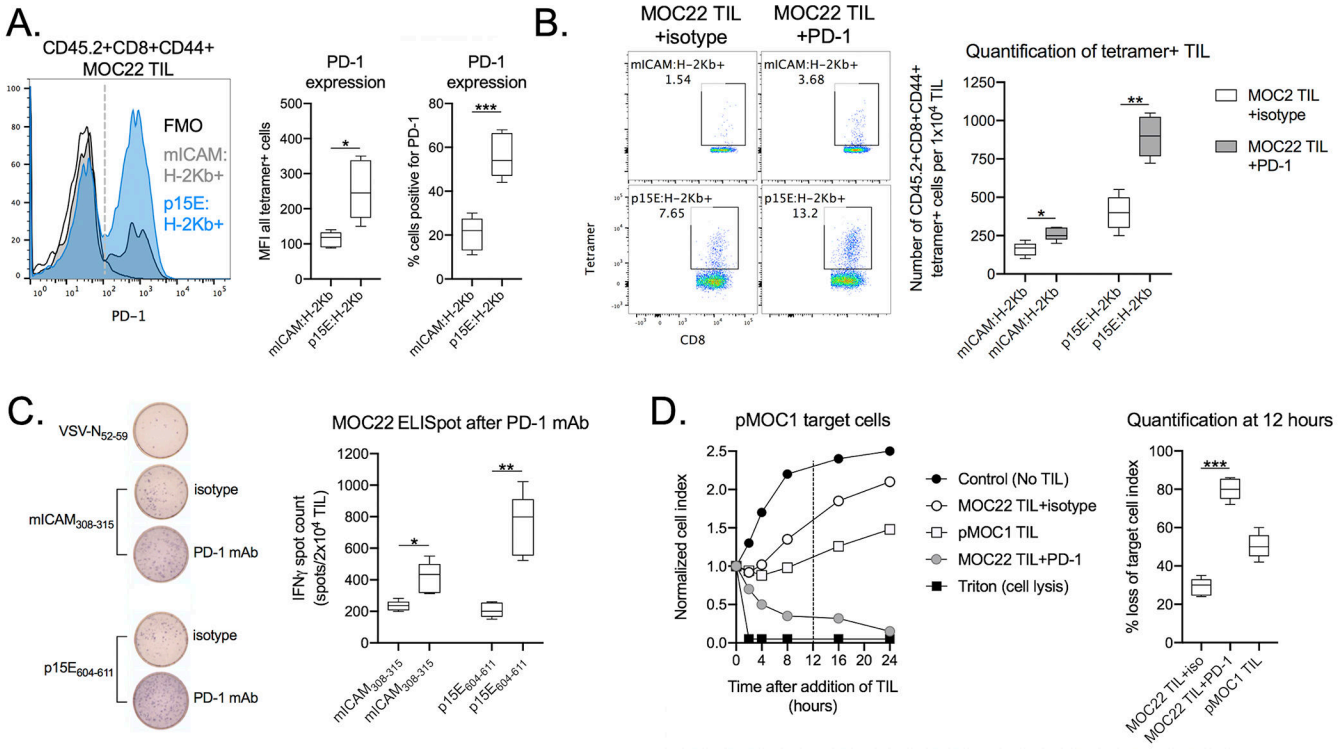

Figure 5 –. PD-1 mAb restored the function of TIL targeting p15E in MOC22 tumors

A, MOC22 TIL specific for OVA:H-2K^b or p15E:H-2K^b were assessed for PD-1 expression by flow cytometry. Representative histogram of PD-1 staining is shown on the left, with qualification of PD-1 expression on all tetramer positive cells (median fluorescent intensity) as well as the percentage of positive cells (dashed grey line) shown on the right.

B, WT B6 mice bearing MOC22 tumors were treated with PD-1 mAb or isotype control (days 7 and 10). TIL were cultured from day 14 tumors, and after 7 days of culture, TIL were assessed for tetramer positivity by flow cytometry. Representative dot plots are shown on the left. Quantity of tetramer positive TIL is shown on the right (n = 5 independent tumors each condition).

C, TIL cultured from day 14 MOC22 tumors treated with PD-1 mAb or isotype control were assessed for IFNγ production upon exposure to antigenic peptides by ELISpot. Representative photomicrographs are shown on the left, with quantification of spot counts on the right (TIL pooled from 5 independent tumors each condition).

D, TIL cultured from day 14 MOC22 tumors treated with PD-1 mAb or isotype control were co-cultured with pMOC1 target cells and loss of target cell viability was assessed by impedance analysis. Representative impedance plot is shown on the left. Quantification of loss of target cell index 12 hours after initiation of co-culture (vertical dashed line) is shown on the right (TIL pooled from 5 independent tumors each condition).

All data shown is representative data from one of at least two independent experiments.

*, $p < 0.05$; **, $p < 0.01$; ***, $p < 0.001$

Author Manuscript Author Manuscript Author Manuscript Author Manuscript

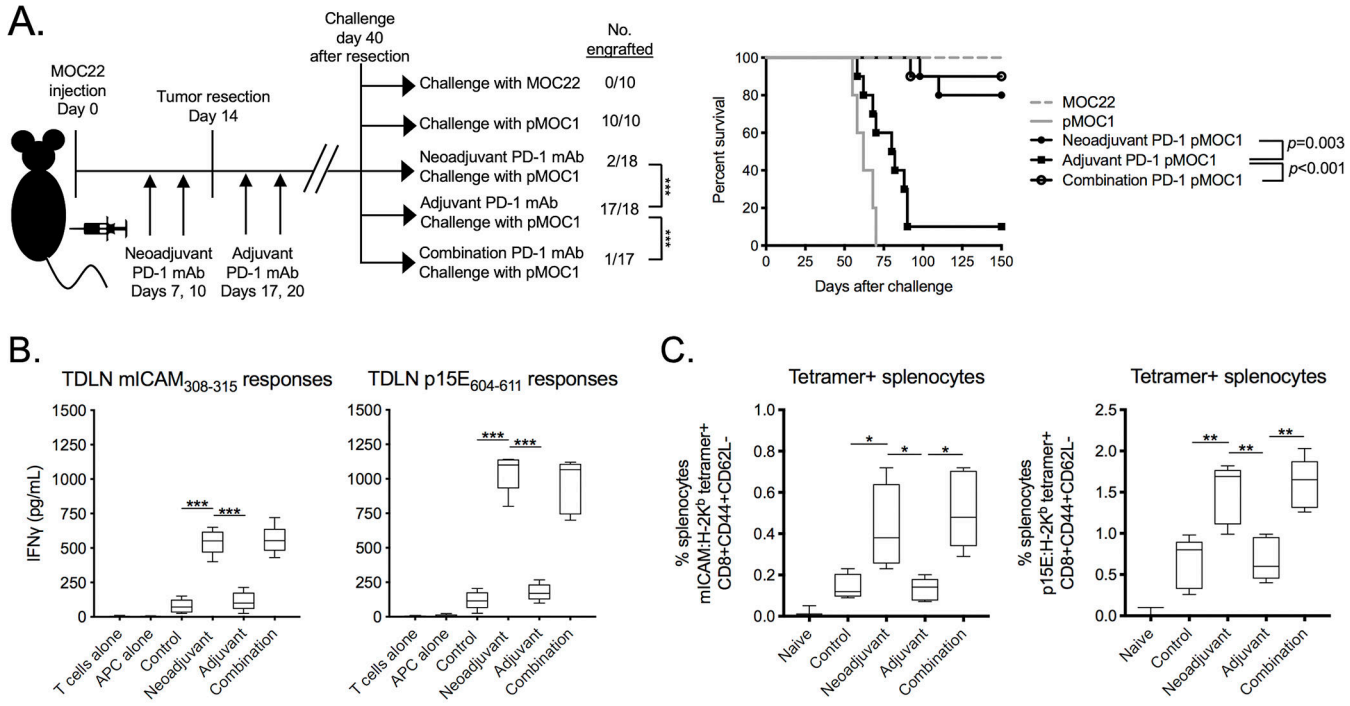

Figure 6 –. Mice rejected engraftment with tumor cells lacking mICAM following neoadjuvant PD-1 mAb

A, MOC22 tumors were established in WT B6 mice and completely resected at day 14. Tumor-bearing mice were given neoadjuvant (days 7 and 10), adjuvant (days 17 and 20) or combination PD-1 mAb. 40 days after resection, untreated mice were challenged with MOC22 or pMOC1 cells as controls, and treated mice were challenged with pMOC1 cells and followed for engraftment. Tumor engraftment rates are shown on the left, and survival to 150 days after challenge is shown as a Kaplan-Meier curve on the right. Cumulative data from two independent experiments.

B and **C**, MOC22 tumor-bearing mice were treated neoadjuvant, adjuvant or combination PD-1 mAb as in A. **B**, 40 days after resection, T cells were sorted form tumor draining lymph nodes (TDLN) and assessed for IFNγ production upon exposure to antigenic peptides by ELISA. **C**, 40 days after resection, splenic T cells were assessed for tetramer and memory marker positivity by flow cytometry ($n = 5$ independent tumors each condition). Unless stated otherwise, all data shown is representative data from one of at least two independent experiments.

*, $p < 0.05$; **, $p < 0.01$; ***, $p < 0.001$